Department of the Navy
Naval Ordnance Test Station
Contract N123(60530)24917A

A THEORETICAL STUDY OF LONGITUDINAL STRAIN PULSE PROPAGATION IN WIDE RECTANGULAR BARS

by

Orval Jones and Albert T. Ellis

Hydrodynamics Laboratory
CALIFORNIA INSTITUTE OF TECHNOLOGY
Pasadena, California

Report No. E-108.14 April 1961

Department of the Navy
Naval Ordnance Test Station
Contract N123(60530)24917A

A THEORETICAL STUDY OF LONGITUDINAL STRAIN PULSE PROPAGATION IN WIDE RECTANGULAR BARS

by

Orval Jones and Albert T. Ellis

Hydrodynamics Laboratory
California Institute of Technology
Pasadena, California

Report No. E-108.14

April 1961

ACKNOWLEDGEMENTS

Financial support from the following sources made this study possible:

1. U. S. Naval Ordnance Test Station Contract N123(60530)24917A.
2. National Science Foundation Grant G-2586.

ABSTRACT

The propagation of a longitudinal elastic strain pulse in a wide rectangular bar is considered on the basis of approximate plane-stress equations of motion. Asymptotic expressions are obtained which, for large distances of travel, describe the pulse propagation in a semi-infinite strip with stress-free lateral edges, subject to the conditions that a uniform normal stress with a step-function time dependence is applied to the end and that the end is laterally constrained. Particular emphasis is given to describing the warping of plane sections during passage of the strain pulse.

INTRODUCTION

In the companion paper, Part II, ultra-high-speed motion pictures are shown of the transient fringe patterns resulting from strain pulse propagation in a rectangular aluminum bar having a birefringent coating. Fringe curvatures observed in these pictures,[3] indicating that plane sections were warping noticeably, provided the motivation for detailed studies of longitudinal strain pulse propagation in rectangular bars.

In this part, Part I, the propagation of a longitudinal strain pulse in a long, thin, wide rectangular bar is considered analytically on the basis of approximate two-dimensional plane-stress equations of motion. Particular emphasis is placed on describing the observed warping of plane sections. The theoretical predictions are compared with experimental results in Part II.

Dispersive transient solutions, based either on exact or approximate equations of motion, for the response of long rectangular bars to extremely high rates of longitudinal loading are apparently not available in the literature. In general, studies on the propagation of longitudinal strain pulses in long bars have dealt only with bars of circular cross-section.[4] This is not surprising since the specification of an additional characteristic length makes the rectangular bar problem an order of magnitude more complicated than the corresponding circular bar problem. It is interesting to note that all of the presently available transient solutions for circular bars are based on the assumption, either explicit or implicit, that plane-sections remain plane during passage of a strain pulse.

Only a very limited amount of experimental and theoretical information is

---

[3] As will be pointed out in Part II, fringe curvatures are present in all the full-field dynamic photoelastic pictures obtained by other investigators for longitudinal impact of rectangular bars of photoelastic material.

[4] See [1][5] for a recent review of work on circular bars.

[5] Numbers in brackets designate References at end of paper.

available on steady-state wave propagation in infinite rectangular bars when the wavelengths are comparable to the cross-sectional dimensions. For a wide rectangular bar (i.e., a bar having a small thickness-to-width ratio) the experimental and theoretical studies of Morse [2,3] indicate that for frequencies below a cut-off frequency no propagation occurs in the lowest thickness mode and that the dispersion of the lowest width mode is generally similar to that predicted by the approximate plane-stress theory [4]. On the basis of the higher order approximate Kane-Mindlin equations of motion [5], Gazis and Mindlin [6] showed that the effect of the lowest symmetric extensional mode across the thickness is to cause the low-frequency long-wavelength velocities of the lowest width mode to be slightly decreased from the corresponding plane-stress values. Recently, Mindlin and Fox [7], using exact elastic equations of motion, obtained solutions for a set of discrete points and associated slopes on branches of the exact frequency spectrum for particular ratios of thickness-to-width. The complete solution was not obtained and it was pointed out that the complete solution cannot be expressed in terms of a finite number of elementary functions. These considerations make an approximate approach to the problem desirable.

STATEMENT OF PROBLEM

For comparison with experimental results presented in Part II, the physical problem to be approximated is the determination of the elastic strains in a long bar of wide rectangular cross-section having stress-free lateral surfaces, subject to the conditions that a uniform normal stress with a step-function time dependence is applied to the end and that the shear stresses applied to the end are zero.

It is assumed that the bar is made of a homogeneous, isotropic, linearly elastic material. The analysis is restricted to a thin, wide rectangular bar which is semi-infinite in length. On the basis of Morse's results, it is assumed that the two-dimensional plane-stress theory (the lowest order approximate

theory that might describe the experimentally observed warping of plane sections) gives a reasonable approximation to the actual bar behavior provided the half-wavelengths involved are greater than the bar width. Due to dispersion this should be the case at the head of the pulse for large distances of travel. Considering only these long-wavelength oscillations at the pulse head for large distances of travel, it is assumed for mathematical simplicity that the nonmixed end conditions stated above can be replaced by mixed end conditions specifying that the applied normal stress (unchanged in magnitude) is uniform and has a step-function time dependence and that the lateral displacement at the end of the bar is zero.[6] Experimental evidence will provide the final test of the validity of these assumptions.

Using rectangular Cartesian coordinates having x along and y at right angles to the centerline of the strip, the plane-stress equations of motion (cf. Love [11], p. 497) written in terms of the areal dilatation Δ and the rotation Ω are

$$\frac{\partial \Delta}{\partial x} - (1 - \sigma)\frac{\partial \Omega}{\partial y} = \frac{\rho(1 - \sigma^2)}{E}\frac{\partial^2 u}{\partial t^2} \tag{1}$$

$$\frac{\partial \Delta}{\partial y} - (1 - \sigma)\frac{\partial \Omega}{\partial x} = \frac{\rho(1 - \sigma^2)}{E}\frac{\partial^2 v}{\partial t^2} \tag{2}$$

where

$$\Delta = \frac{\partial u}{\partial x} + \frac{\partial v}{\partial y} \tag{3}$$

$$\Omega = \frac{1}{2}\left(\frac{\partial v}{\partial x} - \frac{\partial u}{\partial y}\right) \tag{4}$$

In these equations u and v are longitudinal and transverse particle displacements, respectively, t is time, ρ is the material density, E is

---

[6] For the related plane strain problem, Folk [8] has discussed the validity of this assumption in detail. For the analogous circular bar problem, solutions obtained by Folk, Fox, Shook, and Curtis [9] for mixed end conditions were found to be in good agreement for large distances of travel with the experimental results obtained by Fox and Curtis [10] for nonmixed end conditions.

Young's modulus, and σ is Poisson's ratio; Δ and Ω are defined by (3) and (4), respectively.

Solutions to these equations must satisfy the initial conditions

$$u(x,y,0) = v(x,y,0) = \frac{\partial u}{\partial t}(x,y,0) = \frac{\partial v}{\partial t}(x,y,0) = 0 \; ; \tag{5}$$

the boundary conditions at the lateral edges $y = \pm a$ of the strip

$$\tau_{yy}(x, \pm a, t) = \tau_{xy}(x, \pm a, t) = 0; \tag{6}$$

and the input boundary conditions at the end $x = 0$ of the strip

$$\tau_{xx}(0, y, t) = - P_o H(t) \quad \text{and} \quad v(0, y, t) = 0 \tag{7a,b}$$

The displacements must also vanish at infinity. In (7a) P_o denotes the applied pressure and $H(t)$ is the unit step-function.

The stress components τ_{xx}, τ_{yy}, and τ_{xy} are related to the displacements by the following stress-strain relations for plane-stress:

$$\tau_{xx} = \frac{E}{1 - \sigma^2} \left(\frac{\partial u}{\partial x} + \sigma \frac{\partial v}{\partial y} \right) \tag{8}$$

$$\tau_{yy} = \frac{E}{1 - \sigma^2} \left(\frac{\partial v}{\partial y} + \sigma \frac{\partial u}{\partial x} \right) \tag{9}$$

$$\tau_{xy} = \frac{E}{2(1 + \sigma)} \left(\frac{\partial u}{\partial y} + \frac{\partial v}{\partial x} \right) \tag{10}$$

SOLUTION TRANSFORMS

The present boundary value problem lends itself to the double transform method of solution developed by Folk [8,9]. In this method the transforms applied to a particular differential equation are chosen in such a way that only the available initial and end boundary information is required. For comparison with experimental results described in Part II values are required for the strain components e_{xx}, e_{yy}, and e_{xy} where

$$e_{xx} = \frac{\partial u}{\partial x}, \qquad e_{yy} = \frac{\partial v}{\partial y}, \qquad e_{xy} = \frac{\partial v}{\partial x} + \frac{\partial u}{\partial y} \tag{11a,b,c}$$

Let $f^F(x,y,\omega)$, $f^S(\gamma,y,\omega)$, $f^C(\gamma,y,\omega)$ denote Fourier exponential, sine, and cosine transforms, respectively, according to

$$f^F(x,y,\omega) = \int_0^\infty f(x,y,t)\, e^{i\omega t} dt \,, \tag{12a}$$

$$f(x,y,t) = \frac{1}{2\pi} \int_{-\infty + i\varepsilon}^{\infty + i\varepsilon} f^F(x,y,\omega)\, e^{-i\omega t} d\omega \tag{12b}$$

$$f^S(\gamma,y,\omega) = \int_0^\infty f(x,y,\omega) \sin(\gamma x) dx \,, \tag{13a}$$

$$f(x,y,\omega) = -\frac{i}{\pi} \int_{-\infty}^{\infty} f^S(\gamma,y,\omega)\, e^{i\gamma x} d\gamma \tag{13b}$$

$$f^C(\gamma,y,\omega) = \int_0^\infty f(x,y,\omega) \cos(\gamma x) dx \,, \tag{14a}$$

$$f(x,y,\omega) = \frac{1}{\pi} \int_{-\infty}^{\infty} f^C(\gamma,y,\omega)\, e^{i\gamma x} d\gamma \tag{14b}$$

where ω is assumed to have a small, positive imaginary part. Following the general procedure outlined in reference [9], the transformed strain solutions for the present problem are

$$e_{xx}^{SF} = \frac{-2iP_o \sigma (1+\sigma) \gamma^3 (k^2-\gamma^2) \sin(ka)\cos(hy)}{E \omega h^2 F(\gamma,\omega)} + \frac{4iP_o \sigma (1+\sigma) \gamma^3 k \sin(ha)\cos(ky)}{E \omega h F(\gamma,\omega)} + \frac{i(1-\sigma^2)\gamma P_o}{E \omega h^2} \tag{15}$$

$$e_{yy}^{SF} = \frac{-2iP_o \sigma (1+\sigma) \gamma (k^2-\gamma^2) \sin(ka)\cos(hy)}{E \omega F(\gamma,\omega)} - \frac{4iP_o \sigma (1+\sigma) \gamma^3 k \sin(ha)\cos(ky)}{E \omega h F(\gamma,\omega)} \tag{16}$$

$$e_{xy}^{CF} = \frac{4iP_o \sigma (1+\sigma) \gamma^2 (k^2-\gamma^2)}{E \omega h F(\gamma,\omega)} [\sin(ha)\sin(ky) - \sin(ka)\sin(hy)] \tag{17}$$

where

$$F(\gamma,\omega) = (k^2-\gamma^2)^2 \sin(ka)\cos(ha) + 4\gamma^2 h k \sin(ha)\cos(ka) \tag{18}$$

DISCUSSION OF FREQUENCY EQUATION

In the next section the inverse sine and cosine transforms of the strains are obtained by applying the Cauchy residue theorem in the complex γ-plane. Poles of the strain transforms occur for values of γ which satisfy the transcendental

secular equation

$$F(\gamma, \omega) = 0 \tag{19}$$

for a given value of frequency ω . The relevant behavior of the solutions $\gamma = \gamma(\omega)$ of (19) is summarized here.

Equation (19) is the frequency equation for symmetric free vibrations of an infinite elastic strip of vanishing thickness (state of plane-stress). Under the formal transformation $\sigma \to \sigma/(1-\sigma)$ and $E \to E/(1-\sigma^2)$ this equation is identical to the Rayleigh-Lamb frequency equation for symmetric free vibrations of an infinite elastic plate (state of plane-strain). Thus, much of the needed general behavior of the solutions to (19) can be inferred from existing studies of the Rayleigh-Lamb frequency equation, particularly those of Folk [8] and Mindlin and Onoe [12][7]. Specific calculations are carried out when necessary.

For purposes of generality, the following dimensionless variables are introduced:

$$\alpha = \gamma a \qquad \text{and} \qquad \beta = \frac{a\omega}{c_s} \tag{20a,b}$$

where c_s, the shear wave velocity in an infinite medium, is given by $c_s^2 = \frac{E}{2(1+\sigma)\rho}$. In terms of these variables, (19) becomes

$$a^4 F = (\beta^2 - 2\alpha^2)^2 \sin[\beta^2-\alpha^2]^{1/2} \cos[\kappa\beta^2-\alpha^2]^{1/2} + 4\alpha^2[\beta^2-\alpha^2]^{1/2}[\kappa\beta^2-\alpha^2]^{1/2} \sin[\kappa\beta^2-\alpha^2]^{1/2} \cos[\beta^2-\alpha^2]^{1/2} = 0 \tag{21}$$

where $\kappa = \frac{1-\sigma}{2}$.[8] For a specified value of Poisson's ratio, the solutions of (21) determine a countably infinite set of functions $\alpha = \alpha(\beta)$.

It is convenient to use the scheme introduced by Folk [8] for identifying the functions. Consider first the values of $\alpha = \alpha(\beta)$ for $\beta = 0$. The limiting

---

[7] Reference [12] summarizes the studies of Mindlin and his co-workers. In addition it includes an extensive bibliography of other studies.

[8] For the related plane strain case, $\kappa = \frac{1-2\sigma}{2(1-\sigma)}$.

behavior of (21) is

$$\lim_{\beta \to 0} \left[\frac{a^4 F}{i\alpha^2 \beta^2 (\kappa - 1)} \right] = 2\alpha + \sinh 2\alpha = 0 \qquad (22)$$

A root of (22) is identified as $\alpha_{r,s}(0)$ where r orders the root according to its absolute value and s gives its quadrant in the complex α-plane. Roots with larger absolute values are referred to as higher modes. There are four roots with equal magnitudes, one in each quadrant, The only exception is the root $\alpha = 0$. It will be seen later from a series solution for β small, but non-zero, that it is a double root. The root for which $\frac{d\alpha}{d\beta}$ is positive is labelled $\alpha_{1,1}$, the other root is labelled $\alpha_{1,2}$. The functions $\alpha_{r,s}(\beta)$ are defined to be the analytic continuations of the $\alpha_{r,s}(0)$ solutions, and the $\alpha_{r,s}(\beta)$ solutions for $s = 1$ and $s = 2$ are defined to have positive slopes when they are real and positive imaginary components when they are complex or imaginary.

The qualitative behavior of the first two modes, $\alpha_{1,s}$ and $\alpha_{2,s}$, is illustrated in Fig. 1 for real β and $0 < \sigma < 1/2$. For reasons which will become apparent later, the major contributions to the strain solutions are expected to come from these two modes. Since the solutions depend on x being large, contributions due to complex and imaginary roots are unimportant; consequently, accurate calculations are required only for the real roots. Numerical calculations of the values of $\alpha_{1,1}(\beta)$, $\alpha_{2,1}(\beta)$, and $\alpha_{2,2}(\beta)$ in the ranges of β for which these roots are real were made for several values of σ using an IBM 704 computer. The results are partially summarized in Figs. 2 and 3 for $\alpha_{1,1}$ and $\alpha_{2,1}$, respectively, in the regions of positive real β for which the roots are real.

$\alpha_{1,1}(\beta)$ is real for all real values of β. It is a monotonic odd function of β passing through the origin and having a positive slope for all β. To examine the behavior of $\alpha_{1,1}$ for small β, a series expansion $\alpha_{1,1}^2 = \sum_{n=1}^{\infty} A_n \beta^{2n}$ is assumed. Substituting this series into (21), evaluating the first

few coefficients, and taking the square root of the resulting expression gives

$$\alpha_{1,1} = \frac{\beta}{2(1-\kappa)^{1/2}} + \frac{(1-2\kappa)^2\beta^3}{48(1-\kappa)^{3/2}} + \frac{(1-2\kappa)^2}{576(1-\kappa)^{5/2}}\left[\frac{(7-4\kappa^2)}{5} - \frac{(1-2\kappa)^2}{4}\right]\beta^5 + \cdots \tag{23}$$

This series can be used to evaluate $\alpha_{1,1}$ for small β. Knowing the behavior of $\alpha_{1,1}$, $\alpha_{1,2}$ is determined by the relation $\alpha_{1,2}(\beta) = -\alpha_{1,1}(\beta)$.

The second mode solution $\alpha_{2,1}(\beta)$ shown in Fig. 3 has a branch point where $\frac{d\beta}{d\alpha}$ is zero for $\alpha > 0$ which corresponds to the intersection of $\alpha_{2,1}$ and $\alpha_{2,4}$ (see Fig. 1). The real roots at this point join smoothly to the complex roots forming the analytic continuation of the complex root $\alpha_{2,1}(0)$. Points of zero slope also occur for $\alpha = 0$. It has been shown in general (cf. [12]) that complex branches intersect real or imaginary branches at each point for which $\frac{d\beta}{d\alpha}$ is zero. If $\frac{d\beta}{d\alpha}$ is zero for $\alpha = 0$, imaginary branches intersect real branches. The behavior of $\alpha_{2,2}$, $\alpha_{2,3}$, and $\alpha_{2,4}$ can be obtained from the $\alpha_{2,1}$ solution due to the symmetry properties of (21). In the region of β for which the solutions are complex (letting α^* denote the conjugate of α)

$$\alpha_{2,1}(\beta) = -\alpha^*_{2,2}(\beta) = -\alpha_{2,3}(\beta) = \alpha^*_{2,4}(\beta) \tag{24a}$$

When the solutions are imaginary and real, the symmetry conditions and the definitions of the roots when passing through the branch points give

$$\alpha_{2,1}(-\beta) = \alpha_{2,2}(\beta) = \alpha^*_{2,3}(-\beta) = \alpha^*_{2,4}(\beta) \quad \text{for the imaginary} \tag{24b}$$

solutions, and

$$\alpha_{2,1}(\beta) = -\alpha_{2,2}(-\beta) = -\alpha_{2,3}(\beta) = \alpha_{2,4}(-\beta) \quad \text{for the real solutions.} \tag{24c}$$

The behavior of the solutions $\alpha_{r,s}(\beta)$ for $r = 3,4,5,\ldots$ will not be discussed; however, it will be assumed that they can be constructed as the analytic continuations of the $\alpha_{r,s}(0)$ roots according to the definition given above.

Folk [8] has discussed briefly several features of the analytic behavior of solutions to the Rayleigh-Lamb frequency equation when β is complex and his

remarks apply also to solutions of (21). Summarizing, his work indicates that the functions $\alpha_{r,s}$ defined by (21) have no poles in the finite β-plane, probably an infinity of them have essential singularities for β infinite, and all modes except $\alpha_{1,s}$ have branch points along the real β-axis and probably along the imaginary β-axis. For the present problem, it is assumed that $\alpha_{1,1}$ is analytic everywhere in the finite β-plane. For the higher modes, it is assumed that the only singularities are the branch points along the real and imaginary axes, and that analytic functions can be obtained in the regions of interest by appropriate branch cuts.

INVERSION OF TRANSFORMS

The inverse sine transforms of e_{xx}^{SF} and e_{yy}^{SF} and the inverse cosine transform of e_{xy}^{CF} are expressed in integral forms by using (13b) and (14b), respectively.

The resulting integrals are evaluated by applying Cauchy's residue theorem in the complex γ-plane. For each integral the path of integration is closed by adding a semicircle of infinite radius about the origin in the upper half of the complex γ-plane. Since it can be shown in each case that the integral over the semi-circle is zero, the original integral is $2\pi i$ times the sum of the residues of the poles in the upper half of the γ-plane.

If the various trigonometric functions in e_{xx}^{SF} are replaced by their respective infinite series, it is found that only even powers of h and k appear; hence, there are no branch points in the complex γ-plane even though h and k are irrational functions of γ. Similarly, it can be shown that this conclusion is applicable to e_{yy}^{SF} and e_{xy}^{CF}.

Although the functions e_{xx}^{SF}, e_{yy}^{SF}, and e_{xy}^{CF} appear at first glance to have poles for $h = 0$, each function can be defined to be analytic at this point. The only poles of these functions occur for the roots γ which satisfy the frequency equation

$$F(\gamma, \omega) = 0 \tag{19}$$

Since F is a function of both the wave-number γ and the frequency ω, the position of a pole in the γ-plane depends on the value used for ω. When the frequency is real, the number of poles lying on the real γ-axis depends on the value of ω. However, the inverse Fourier transforms involve slightly complex frequencies, that is, $\omega = \omega_o + i\varepsilon$ where ε is a vanishingly small but positive number and real ω_o varies from $-\infty$ to $+\infty$. The real roots $\gamma_{r,s}(= a_{r,s}/a)$ of (21) when the frequency is real are shifted to slightly complex roots when the frequency is in this range. By expanding $\gamma_{r,s}$ in a Taylor series about ω_o, it can be shown for ε very small and positive that the imaginary part of $\gamma_{r,s}(\omega_o + i\varepsilon)$ is positive or negative according to the sign of $\frac{d\gamma_{r,s}}{d\omega}$ evaluated for $\omega = \omega_o$. The functions $\gamma_{r,s}$ were defined so that the roots in the upper and lower halves of the γ-plane remain in the upper and lower halves, respectively, as ω_o varies from $-\infty$ to $+\infty$. Thus, when the frequency is in the range noted above, the roots of (21) are all single and no roots lie on the real axis.

Since $\gamma_{r,1}$ and $\gamma_{r,2}$ are always in the upper half of the γ-plane, the residue summations for the integrals will include only roots for which $s = 1$ or 2. There is one exception to this rule: $\gamma_{1,1}$ is included but $\gamma_{1,2}$ is not. Taking the residues of the poles according to this rule and multiplying by $2\pi i$, e^F_{xx} becomes

$$e^F_{xx}(x,y,\omega) = i\frac{P_o}{E}\sum_{r,s}\phi_{xx}(\gamma_{r,s},y,\omega)\,e^{i\gamma_{r,s}x} \tag{25a}$$

where

$$\phi_{xx}(\gamma_{r,s},y,\omega) = \frac{4\sigma(1+\sigma)\gamma^3}{\omega h^2\frac{\partial F}{\partial\gamma}}\Big[2hk\sin(ha)\cos(ky) - (k^2-\gamma^2)\sin(ka)\cos(hy)\Big]\Big|_{\gamma=\gamma_{r,s}} \tag{25b}$$

Similarly,

$$e^F_{yy}(x,y,\omega) = -\frac{i\sigma P_o}{E}\sum_{r,s}\phi_{yy}(\gamma_{r,s},y,\omega)e^{i\gamma_{r,s}x} \tag{26a}$$

where

$$\phi_{yy}(\gamma_{r,s},y,\omega) = \frac{4(1+\sigma)\gamma}{\omega \frac{\partial F}{\partial \gamma}} \left[(k^2 - \gamma^2)\sin(ka)\cos(hy) \right.$$

$$\left. + 2\gamma^2 \frac{k}{h} \sin(ha)\cos(ky) \right] \Bigg|_{\gamma = \gamma_{r,s}} \tag{26b}$$

and

$$e^F_{xy}(x,y,\omega) = \frac{P_o}{E} \sum_{r,s} \phi_{xy}(\gamma_{r,s},y,\omega) e^{i\gamma_{r,s}x} \tag{27a}$$

where

$$\phi_{xy}(\gamma_{r,s},y,\omega) = \frac{-8\sigma(1+\sigma)\gamma^2}{\omega h \frac{\partial F}{\partial \gamma}} (k^2 - \gamma^2) \left[\sin(ha)\sin(ky) \right.$$

$$\left. - \sin(ka)\sin(hy) \right] \Bigg|_{\gamma = \gamma_{r,s}} \tag{27b}$$

The formal expressions for the strains are obtained by taking the inverse Fourier transforms according to (12b) of e^F_{xx}, e^F_{yy}, and e^F_{xy}. Introducing the dimensionless variables

$$T = \frac{c_s t}{a}, \qquad X = \frac{x}{a}, \qquad \text{and} \qquad Y = \frac{y}{a} \tag{28a,b,c}$$

in addition to α and β defined by (20a,b), the strains are

$$e_{xx}(X,Y,T) = \sum_{r,s} (e_{xx})_{r,s} \equiv$$

$$= -\frac{P_o}{E} \sum_{r,s} \frac{1}{2\pi i} \int_{-\infty+i\varepsilon}^{\infty+i\varepsilon} \theta_{xx}(\alpha_{r,s},Y,\beta) e^{i(\alpha_{r,s}X - \beta T)} d\beta \tag{29}$$

$$e_{yy}(X,Y,T) = \sum_{r,s} (e_{yy})_{r,s} \equiv$$

$$= \frac{\sigma P_o}{E} \sum_{r,s} \frac{1}{2\pi i} \int_{-\infty+i\varepsilon}^{\infty+i\varepsilon} \theta_{yy}(\alpha_{r,s},Y,\beta) e^{i(\alpha_{r,s}X - \beta T)} d\beta \tag{30}$$

$$e_{xy}(X,Y,T) = \sum_{r,s} (e_{xy})_{r,s} \equiv$$

$$= \frac{P_o}{E} \sum_{r,s} \frac{i}{2\pi i} \int_{-\infty+i\varepsilon}^{\infty+i\varepsilon} \theta_{xy}(\alpha_{r,s},Y,\beta) e^{i(\alpha_{r,s}X - \beta T)} d\beta \tag{31}$$

where

$$\theta_{xx} = (c_s/a)\,\phi_{xx}, \quad \theta_{yy} = (c_s/a)\,\phi_{yy}, \quad \theta_{xy} = (c_s/a)\,\phi_{xy} \tag{32a,b,c}$$

The terms $(e_{xx})_{r,s}$, $(e_{yy})_{r,s}$, and $(e_{xy})_{r,s}$ are defined in (29), (30), and (31), respectively.

EVALUATION OF STRAIN INTEGRALS FOR LARGE DISTANCES OF TRAVEL

Due to the complexity of Θ_{xx}, Θ_{yy}, Θ_{xy} and the functions $\alpha_{r,s}$, the integrals of (29), (30), and (31) cannot in general be evaluated by simple means. However, by using saddle point methods (see, for example, [13] and [14]), it is possible to obtain asymptotic expressions which are valid for large values of X. The use of such methods is appropriate in the present problem since only for large values of X can the approximate theory and the assumption made concerning the end conditions be expected to give reasonable results.

Saddlepoint methods for evaluating such integrals are based on the concept of deforming the original path of integration in the complex β-plane to pass through the saddlepoints in the direction of steepest descent; thus, the major contributions to an integral come from portions of the path in the neighborhoods of the saddlepoints and from any poles that are crossed in deforming the path. The saddlepoints are defined by

$$\frac{d\alpha_{r,s}}{d\beta} = \frac{T}{X} \tag{33}$$

For fixed X and given T, saddlepoint values of $\alpha_{r,s}$ and β, denoted by $\bar{\alpha}_{r,s}$ and $\bar{\beta}$, satisfy equation (21) subject to condition (33). The position of a saddlepoint in the complex β-plane is given by $\bar{\beta}$. Because of the time dependent behavior of the saddlepoints the same approximation cannot be used to describe all portions of the pulse.

For the ordinary saddlepoint (OSP) approximation, second order saddlepoints ($\bar{\alpha}''_{r,s} \neq 0$) are widely separated and the integrand functions are expanded in series about the moving saddlepoints (see [13] for details). In this approximation, $X|\bar{\alpha}''_{r,s}|$ must be large in order that the main contribution to an integral will be concentrated about the saddle point. At certain times, however, the second order

saddlepoints collide to form third order saddlepoints ($\bar{\alpha}''_{r,s} = 0$). Consequently, during the time interval when the saddlepoints are close together, the OSP method is inapplicable. An extended saddle point (ESP) approximation is used to evaluate the integrals during these time intervals. In this approximation the integrand functions are expanded in series about the collision point in the β-plane where $\bar{\alpha}''_{r,s}$ is zero. Special cases occur when there are zeros and/or poles of the integrand functions $\Theta(\alpha_{r,s}, Y, \beta)$ near saddlepoints (see [14] for details).

FIRST MODE STRAIN CONTRIBUTIONS. The integrals $(e_{xx})_{1,1}$, $(e_{yy})_{1,1}$, and $(e_{xy})_{1,1}$ are evaluated quantitatively only when the saddlepoints lie on the real β axis. Mathematical expressions are obtained which describe the major features of the head of the pulse observed at station X as time T progresses.

In order to determine during what time intervals a particular approximation can be used, it is necessary to examine the first mode saddle point behavior in the complex β-plane as a function of time T. First mode saddle points are defined by $\alpha'_{1,1} = T/X$. $\alpha'_{1,1}$ is plotted for real β in Fig. 2 and (23) can be used to evaluate the derivative when β is slightly imaginary. As mentioned previously, a complete description of $\alpha_{1,1}$ for complex β is not available.

The first large signal to arrive at a fixed station X corresponds to the collision of two second order saddle points at the origin for $T/X = [2 + 2\sigma]^{-1/2}$. For times just prior to the formation of this third order saddlepoint, calculations from (23) indicate that the two saddlepoints were moving along the imaginary axis toward the origin. It can also be shown from (23) that $i(\bar{\alpha}_{1,1}X - \bar{\beta}\,T)$ is negative as the saddle points approach the origin; therefore, for large X the initial signal is expected to be very small and probably has a time dependence of the form $e^{-\zeta}$, where ζ decreases as T/X approaches $[2 + 2\sigma]^{-1/2}$. As T/X increases from its collision value the third order saddlepoint separates into two second order saddle points moving apart on the real β axis (cf. Fig. 2).

The ESP method is used to describe the strains during the collision process. The approximations for Θ_{xx}, Θ_{yy}, Θ_{xy}, and $(\alpha_{1,1}X - \beta T)$ are taken as

$$\Theta_{xx}(\alpha_{1,1},Y,\beta) \cong -\frac{1}{\beta} - \frac{1}{(1+\sigma)}\left[\frac{\sigma}{4}(1-Y^2) - \frac{\sigma(1-\sigma)}{6}\right]\beta - \left[\eta_x(\sigma) - \upsilon_x(\sigma)(1-Y^2) - \chi_x(\sigma)Y^2(1-\psi_x(\sigma)Y^2)\right]\beta^3 \tag{34}$$

$$\Theta_{yy}(\alpha_{1,1},Y,\beta) \cong -\frac{1}{\beta} - \frac{1}{(1+\sigma)}\left[\frac{(1+\sigma-\sigma^2)}{4}(1-Y^2) - \frac{\sigma(1-\sigma)}{6}\right]\beta - \left[\eta_y(\sigma) - \upsilon_y(\sigma)(1-Y^2) - \chi_y(\sigma)Y^2(1-\psi_y(\sigma)Y^2)\right]\beta^3 \tag{35}$$

$$\Theta_{xy}(\alpha_{1,1},Y,\beta) \cong \frac{\sigma^2 Y(1-Y^2)\beta^2}{6(2+2\sigma)^{1/2}} \tag{36}$$

and

$$\alpha_{1,1}X - \beta T \cong \left[\frac{X}{(2+2\sigma)^{1/2}} - T\right]\beta + \frac{\sigma^2 X}{6(2+2\sigma)^{3/2}}\beta^3 \tag{37}$$

where the values of η_x, υ_x, χ_x, and ψ_x and of η_y, υ_y, χ_y, and ψ_y are to be taken from Figs. 4 and 5, respectively, for a specified value of σ. The series for Θ_{xx}, Θ_{yy}, and Θ_{xy} were obtained by substituting (23) into (32a,b,c) and retaining only the first few terms.

Using these approximations, the ESP method gives the following expressions for the first mode strains:

$$(e_{xx})_{1,1} \cong -\frac{P_o}{E}\left\{\left[\frac{1}{3} + \int_0^B Ai(-\xi)d\xi\right] - \left[\frac{\sigma}{2}(1-Y^2) - \frac{\sigma(1-\sigma)}{3}\right]\left[\frac{2}{\sigma^2 X}\right]^{2/3}\frac{dAi(-B)}{dB} + 4(1+\sigma)^2\left[\eta_x(\sigma) - \upsilon_x(\sigma)(1-Y^2) - \chi_x(\sigma)Y^2(1-\psi_x(\sigma)Y^2)\right]\left[\frac{2}{\sigma^2 X}\right]^{4/3}\frac{d^3Ai(-B)}{dB^3}\right\} \tag{38}$$

$$(e_{yy})_{1,1} \cong \frac{\sigma P_o}{E}\left\{\left[\frac{1}{3} + \int_0^B \mathrm{Ai}(-\xi)d\xi\right]\right.$$

$$- \left[\frac{(1+\sigma-\sigma^2)}{2}(1-Y^2) - \frac{\sigma(1-\sigma)}{3}\right]\left[\frac{2}{\sigma^2 X}\right]^{2/3}\frac{d\mathrm{Ai}(-B)}{dB}$$

$$+ 4(1+\sigma)^2\left[\eta_y(\sigma) - \upsilon_y(\sigma)(1-Y^2) - \chi_y(\sigma)Y^2(1-\psi_y(\sigma)Y^2)\right]$$

$$\left.\cdot\left[\frac{2}{\sigma^2 X}\right]^{4/3}\frac{d^3\mathrm{Ai}(-B)}{dB^3}\right\} \tag{39}$$

$$(e_{xy})_{1,1} \cong -\frac{P_o}{E}\,\frac{2}{3}\,\frac{(1+\sigma)}{X}\,Y(1-Y^2)\,\frac{d^2\mathrm{Ai}(-B)}{dB^2} \tag{40}$$

where

$$B = (2+2\sigma)^{1/2}\left[\frac{2}{\sigma^2 X}\right]^{1/3}\left[T - \frac{X}{(2+2\sigma)^{1/2}}\right] \tag{41}$$

The Airy function $\mathrm{Ai}(z)$, its integral, and first three derivatives are shown in Figs. 6 and 7.

It should be noted in passing that the only terms in the expressions for $(e_{xx})_{1,1}$, $(e_{yy})_{1,1}$ and $(e_{xy})_{1,1}$ which do not decrease as X increases are the initial terms in $(e_{xx})_{1,1}$ and $(e_{yy})_{1,1}$. In the limit as X becomes very large $(e_{yy})_{1,1} = -\sigma(e_{xx})_{1,1}$, independent of Y, and $(e_{xy})_{1,1}$ vanishes. This result is expected on physical grounds.

After the two second order saddlepoints have become sufficiently separated on the real β axis, the strains are approximated using the OSP method. Approximating the amplitude factors Θ_{xx}, Θ_{yy}, and Θ_{xy} by their values at the saddlepoints and retaining only terms through second order in β in the series expansion for $(\alpha_{1,1}X - \beta T)$, the resulting expressions for the initial two ordinary saddlepoints on the real β axis are

$$(e_{xx})_{1,1} = -\frac{P_o}{E}\left[1 + \frac{2\Theta_{xx}(\bar{\alpha}_{1,1}, Y, \bar{\beta})}{(2\pi X|\bar{\alpha}''_{1,1}|)^{1/2}}\sin(\bar{\alpha}_{1,1}X - \bar{\beta}T + \tfrac{\pi}{4})\right] \tag{42}$$

$$(e_{yy})_{1,1} \cong \frac{\sigma P_o}{E}\left[1 + \frac{2\Theta_{yy}(\bar{\alpha}_{1,1}, Y, \bar{\beta})}{(2\pi X|\bar{\alpha}''_{1,1}|)^{1/2}} \sin(\bar{\alpha}_{1,1}X - \bar{\beta}\ T + \tfrac{\pi}{4})\right] \tag{43}$$

$$(e_{xy})_{1,1} \cong \frac{2P_o}{E} \frac{\Theta_{xy}(\bar{\alpha}_{1,1}, Y, \bar{\beta})}{(2\pi X|\bar{\alpha}''_{1,1}|)^{1/2}} \cos(\bar{\alpha}_{1,1}X - \bar{\beta}\ T + \tfrac{\pi}{4}) \tag{44}$$

These expressions predict that at a time $T = X\bar{\alpha}'_{1,1}$ there will be oscillations having an instantaneous period $(2\pi a)/(c_s \bar{\beta})$, a wavelength $2\pi a/\bar{\alpha}_{1,1}$, and an amplitude that descreases with increasing X as $X^{-1/2}$. The amplitudes of the oscillations are easily computed for given values of σ and Y by using the values of $\Theta_{xx}(\bar{\alpha}_{1,1}, Y, \bar{\beta})$, $\Theta_{yy}(\bar{\alpha}_{1,1}, Y, \bar{\beta})$, and $\Theta_{xy}(\bar{\alpha}_{1,1}, Y, \bar{\beta})$ obtained from Fig. 8 and the values of $\bar{\alpha}''_{1,1}(\beta)$ obtained from Fig. 2. The static strain values in the expressions for $(e_{xx})_{1,1}$ and $(e_{yy})_{1,1}$ result from deforming the contours across the poles of Θ_{xx} and Θ_{yy} at the origin.

HIGHER MODE STRAIN CONTRIBUTIONS. As β increases, the solutions $\alpha_{1,2}$ and $\alpha_{2,2}$ are the first solutions to become real; hence the second mode terms are expected to be next in importance to the first mode terms. The remaining higher modes are expected to contribute oscillations which are smaller than those of the second mode.

The integrals $(e_{xx})_{2,1}$ and $(e_{xx})_{2,2}$ are complex conjugates which combine to give a real contribution to the strain signal; this is also true of $(e_{yy})_{2,1} + (e_{yy})_{2,2}$ and $(e_{xy})_{2,1} + (e_{xy})_{2,2}$.[9] The second mode contributions will be approximately evaluated for a short time interval which includes the first and largest signals arising from the $\alpha_{2,1}$ and $\alpha_{2,2}$ roots.[10] Second order saddlepoints for $\alpha_{2,1}$ and $\alpha_{2,2}$ are at complex values of β for $T/X < (\alpha'_{2,1})_{min.} = (\alpha'_{2,2})_{min.}$, and so signals approach zero exponentially for large X

---

[9] These sums, for all time, correspond to the contributions from what is classically termed the second and third modes.

[10] The strains from these initial saddlepoints correspond to contributions from what is classically termed the second mode.

until an interval just prior to this time. For $T/X = (\alpha'_{2,1})_{min.}$, two second order saddle points collide on the positive real β-axis to form third order saddlepoints. As time increases the saddlepoints separate and travel apart in opposite directions on the positive real β-axis (cf. Fig. 3). Due to the symmetry of the frequency equation identical behavior takes place on the negative real β-axis.

The ESP method is used to approximate the strains when the saddle points are close together. Approximating the amplitude factors θ_{xx}, θ_{yy}, and θ_{xy} by their values at the collision points and retaining terms through third order in β in the series expansions for $(\alpha_{2,s}X - \beta T)$ about the collision points, the resulting expressions are

$$(e_{xx})_{2,1} + (e_{xx})_{2,2} = -\frac{2P_o}{E}\theta_{xx}(\bar{\alpha}_{2,1}, Y, \bar{\beta})\left(\frac{2}{X|\bar{\alpha}'''_{2,1}|}\right)^{1/3} \cdot \mathrm{Ai}\left[(\bar{\alpha}'_{2,1}X - T)\left(\frac{2}{X|\bar{\alpha}'''_{2,1}|}\right)^{1/3}\right]\sin(\bar{\alpha}_{2,1}X - \bar{\beta}T) \qquad (45)$$

$$(e_{yy})_{2,1} + (e_{yy})_{2,2} = \frac{2\sigma P_o}{E}\theta_{yy}(\bar{\alpha}_{2,1}, Y, \bar{\beta})\left(\frac{2}{X|\bar{\alpha}'''_{2,1}|}\right)^{1/3} \cdot \mathrm{Ai}\left[(\bar{\alpha}'_{2,1}X - T)\left(\frac{2}{X|\bar{\alpha}'''_{2,1}|}\right)^{1/3}\right]\sin(\bar{\alpha}_{2,1}X - \bar{\beta}T) \qquad (46)$$

and

$$(e_{xy})_{2,1} + (e_{xy})_{2,2} = \frac{2P_o}{E}\theta_{xy}(\bar{\alpha}_{2,1}, Y, \bar{\beta})\left(\frac{2}{X|\bar{\alpha}'''_{2,1}|}\right)^{1/3} \cdot \mathrm{Ai}\left[(\bar{\alpha}'_{2,1}X - T)\left(\frac{2}{X|\bar{\alpha}'''_{2,1}|}\right)^{1/3}\right]\cos(\bar{\alpha}_{2,1}X - \bar{\beta}T) \qquad (47)$$

During the time interval when there are four sufficiently separated ordinary saddlepoints, the expressions become

$$(e_{xx})_{2,1} + (e_{xx})_{2,2} = -\frac{2P_o}{E}\sum_{i=1}^{2}\frac{\theta_{xx}(\bar{\alpha}_{2,1}, Y, \bar{\beta}_i)}{(2\pi X|\bar{\alpha}''_{2,1}|)^{1/2}}$$

$$\cdot \sin(\bar{\alpha}_{2,1}X - \bar{\beta}_i T + \tfrac{\pi}{4}\operatorname{sgn}\bar{\alpha}''_{2,1}) \tag{48}$$

$$(e_{yy})_{2,1} + (e_{yy})_{2,2} = \frac{2\sigma P_o}{E}\sum_{i=1}^{2}\frac{\theta_{yy}(\bar{\alpha}_{2,1}, Y, \bar{\beta}_i)}{(2\pi X|\bar{\alpha}''_{2,1}|)^{1/2}}$$

$$\cdot \sin(\bar{\alpha}_{2,1}X - \bar{\beta}_i T + \tfrac{\pi}{4}\operatorname{sgn}\bar{\alpha}''_{2,1}) \tag{49}$$

and

$$(e_{xy})_{2,1} + (e_{xy})_{2,2} = \frac{2P_o}{E}\sum_{i=1}^{2}\frac{\theta_{xy}(\bar{\alpha}_{2,1}, Y, \bar{\beta}_i)}{(2\pi X|\bar{\alpha}''_{2,1}|)^{1/2}}$$

$$\cdot \cos(\bar{\alpha}_{2,1}X - \bar{\beta}_i T + \tfrac{\pi}{4}\operatorname{sgn}\bar{\alpha}''_{2,1}) \tag{50}$$

where all quantities are evaluated for positive β. Values for $\theta_{xx}(\bar{\alpha}_{2,1}, Y, \bar{\beta})$, $\theta_{yy}(\bar{\alpha}_{2,1}, Y, \bar{\beta})$, $\theta_{xy}(\bar{\alpha}_{2,1}, Y, \bar{\beta})$, and $\bar{\alpha}''_{2,1}(\beta)$ are given for several values of σ in Figs. 9 and 3.

The total strains e_{xx}, e_{yy}, e_{xy} include the contributions from all modes. From the sketch given by Mindlin [12], it can be seen that the minimum value of $d\alpha/d\beta$ is larger for the next few roots above $\alpha_{1,1}$ and $\alpha_{2,1}$ and it occurs for larger values of $|\beta|$. Thus, these higher modes will contribute smaller oscillations at later times. However, Folk [8] points out that some of the roots $\alpha_{r,s}$ for r large can have minimum values of $d\alpha/d\beta$ corresponding to signals travelling at dilatation velocity. Mindlin's sketch corroborates this observation. These minimums occur, however, for very large values of $|\beta|$ and result in oscillations of negligible amplitude for the present problem. In problems where the Fourier transform of the end input is large for these large values of β (e.g. a delta function input), the higher modes might contribute a finite signal travelling at the dilatation velocity.

REMARKS. The physical significance of the strain expressions which have been developed will be examined in connection with experimental results in the

companion paper, Part II.

By introducing the transformation $\sigma \rightarrow \sigma/1-\sigma$ and $E \rightarrow E/1-\sigma^2$, all of the results obtained here are applicable to the related plane strain problem of a semi-infinite slab with stress-free lateral surfaces subject to the edge conditions that the stress applied normally is uniform with a step function time dependence and that the lateral edge displacement is zero. Folk [8] considered this problem and obtained solutions for the stress τ_{xx} at the surface of a slab for which $\sigma = 1/3$; however, he did not consider the distribution of stress or strain across the slab thickness.

The solutions given here to the plane-stress problem should approximately describe the behavior of a wide rectangular bar when the wavelength is greater than the bar width. However, for the plane-strain problem the solutions are not subject to such a restriction since they arise from the exact equations of motion for the slab.

REFERENCES

1 J. Miklowitz, "Recent Developments in Elastic Wave Propagation," Applied Mechanics Reviews, vol. 13, 1960, pp. 865-878.

2 R. W. Morse, "Dispersion of Compressional Waves in Isotropic Rods of Rectangular Cross Section," Journal of the Acoustical Society of America, vol. 20, 1948, pp. 833-838.

3 R. W. Morse, "The Velocity of Compressional Waves in Rods of Rectangular Cross Section," Journal of the Acoustical Society of America, vol. 22, 1950, pp. 219-223.

4 R. E. D. Bishop, "On Dynamical Problems of Plane Stress and Plane Strain," Quarterly Journal of Mechanics and Applied Mathematics, vol. 6, 1953, pp. 250-254.

5 T. R. Kane and R. D. Mindlin, "High-Frequency Extensional Vibrations of Plates," Journal of Applied Mechanics, vol. 23, Trans. ASME, vol. 78, 1956, pp. 277-283.

6 D. C. Gazis and R. D. Mindlin, "Influence of Width on Velocities of Long Waves in Plates," Journal of Applied Mechanics, vol. 24, Trans. ASME, vol. 79, 1957, pp. 541-546.

7 R. D. Mindlin and E. A. Fox, "Vibrations and Waves in Elastic Bars of Rectangular Cross Section," Journal of Applied Mechanics, vol. 27, Trans. ASME, vol. 82, Series E, 1960, pp. 152-158.

8 R. T. Folk, "Time Dependent Boundary Value Problems in Elasticity," Ph.D. Dissertation, Lehigh University, Bethlehem, Pa., 1958.

9 R. Folk, G. Fox, C. A. Shook, and C. W. Curtis, "Elastic Strain Produced by Sudden Application of Pressure to One End of a Cylindrical Bar. I. Theory," Journal of the Acoustical Society of America, vol. 30, 1958, pp. 552-558.

10 G. Fox and C. W. Curtis, "Elastic Strain Produced by Sudden Application of Pressure to One End of a Cylindrical Bar. II. Experimental Observations," Journal of the Acoustical Society of America, vol. 30, 1958, pp. 559-563.

11 A. E. H. Love, "A Treatise on the Mathematical Theory of Elasticity," Cambridge University Press, London, Fourth Edition, 1927.

12 R. D. Mindlin, "Waves and Vibrations in Isotropic, Elastic Plates," Structural Mechanics, Proceedings of the First Symposium on Naval Structural Mechanics, Pergamon Press, New York, 1960, pp. 199-232.

13 H. and B. S. Jeffreys, "Methods of Mathematical Physics," Cambridge University Press, Cambridge, England, third edition, 1956, chapter 17.

14 M. V. Cerrillo, "An Elementary Introduction to the Theory of the Saddle-point Method of Integration," Technical Report No. 55:2a, Research Laboratory of Electronics, Massachusetts Institute of Technology, Cambridge, Mass. 1950.

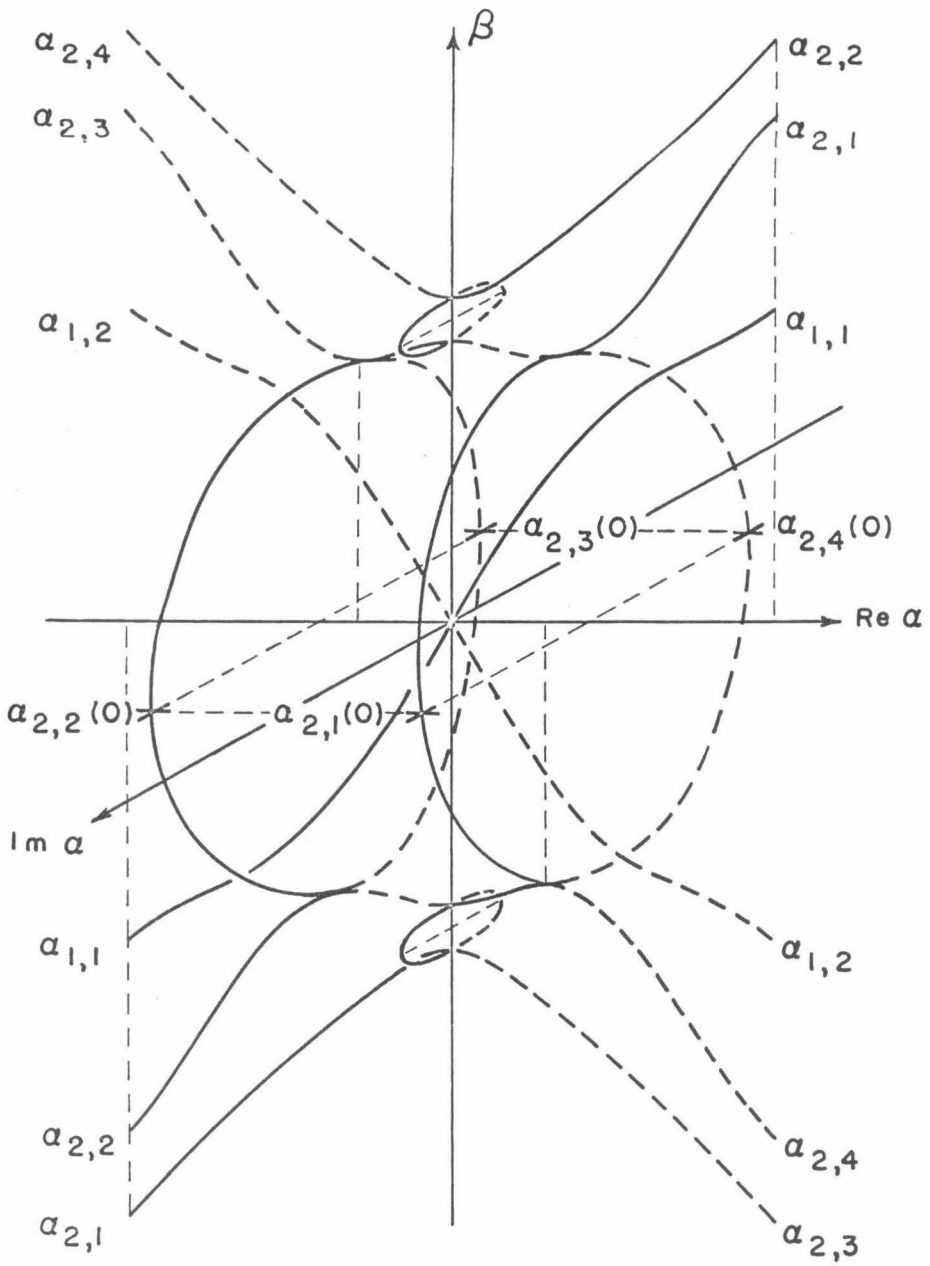

Figure 1.

Qualitative behavior of functions $\alpha_{1,s}$ and $\alpha_{2,s}$ for real β and $0 < \sigma < 1/2$

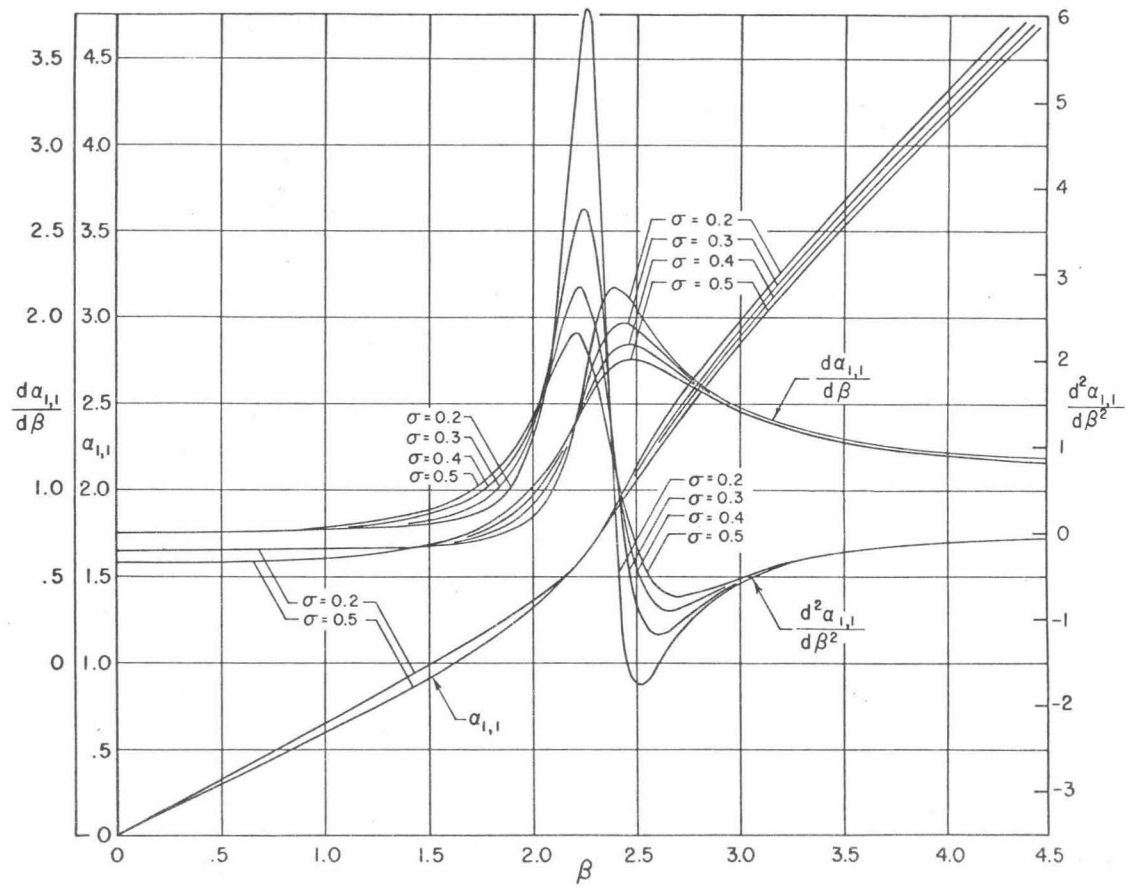

Figure 2.

Function $\alpha_{1,1}(\beta)$ and its first two derivatives for real positive β and $\sigma = 0.2, 0.3, 0.4,$ and 0.5

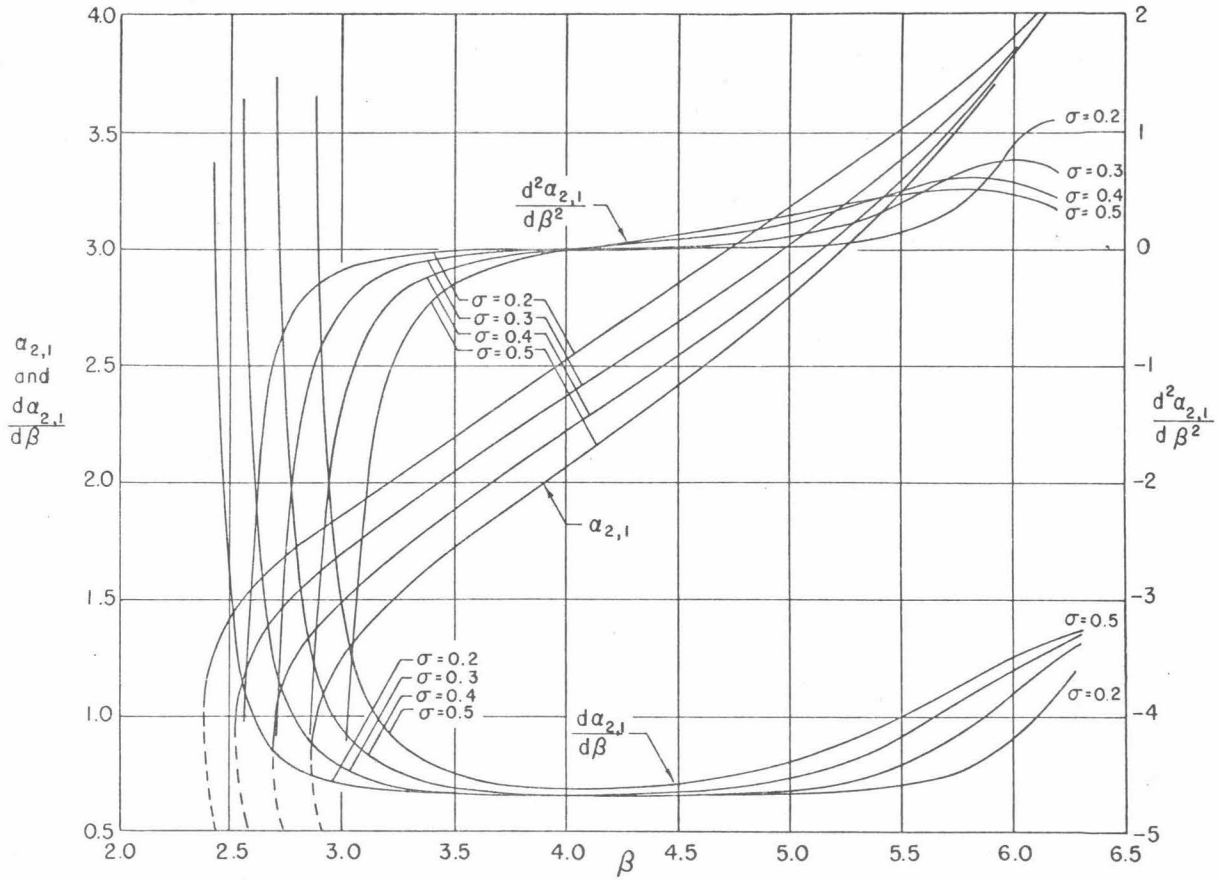

Figure 3.

Function $\alpha_{2,1}(\beta)$ and its first two derivatives in region of real positive β corresponding to real $\alpha_{2,1}$ for σ = 0.2, 0.3, 0.4, and 0.5

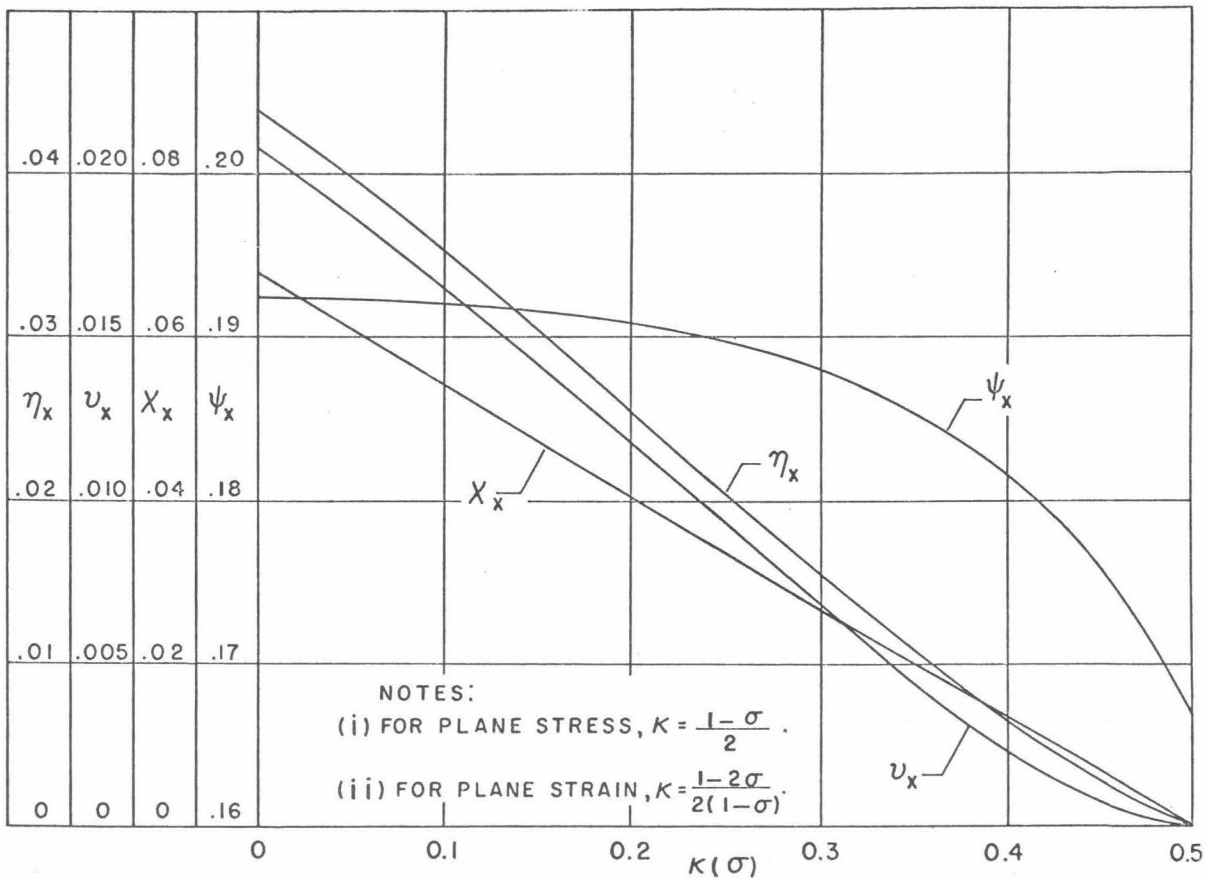

Figure 4.

Coefficients η_x, υ_x, χ_x, and ψ_x as functions of $\kappa(\sigma)$

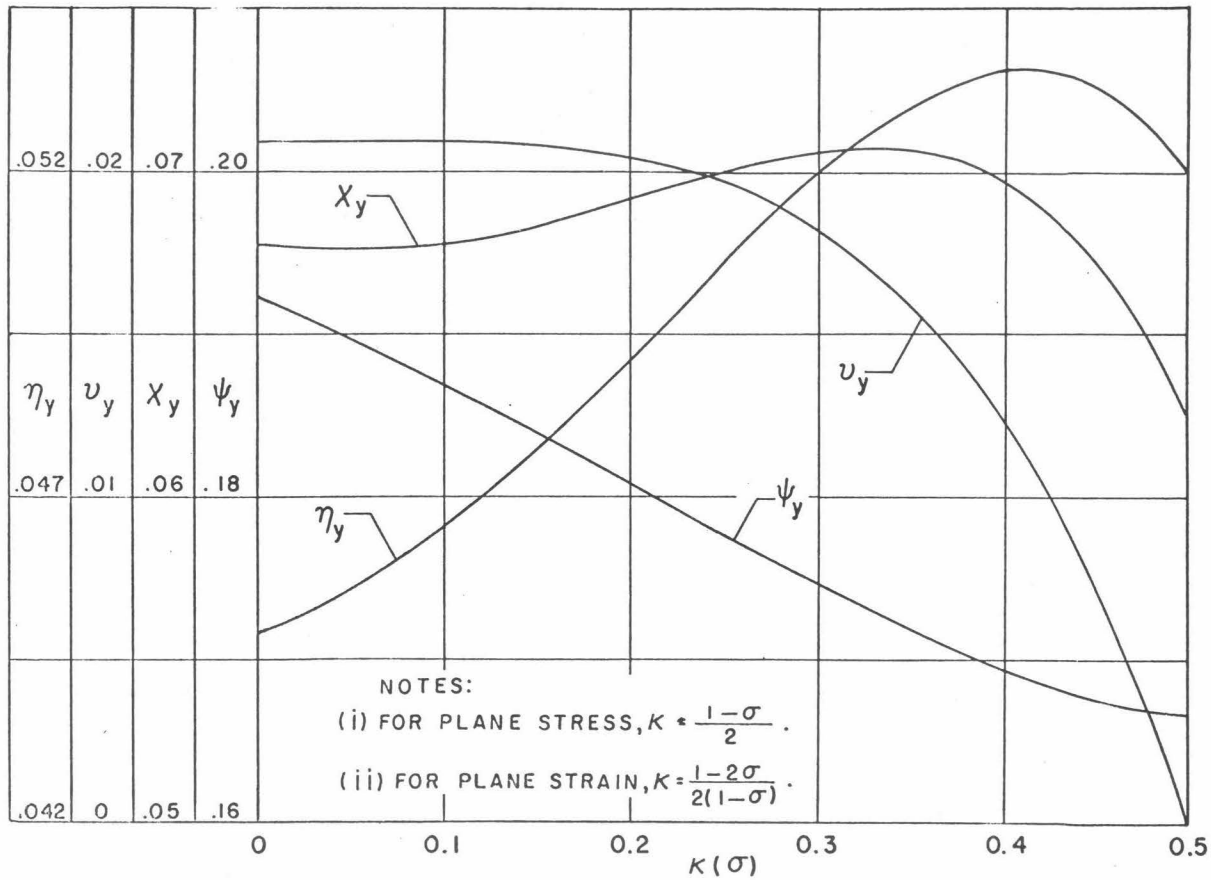

Figure 5.

Coefficients η_y, υ_y, χ_y, and ψ_y as functions of $\kappa(\sigma)$

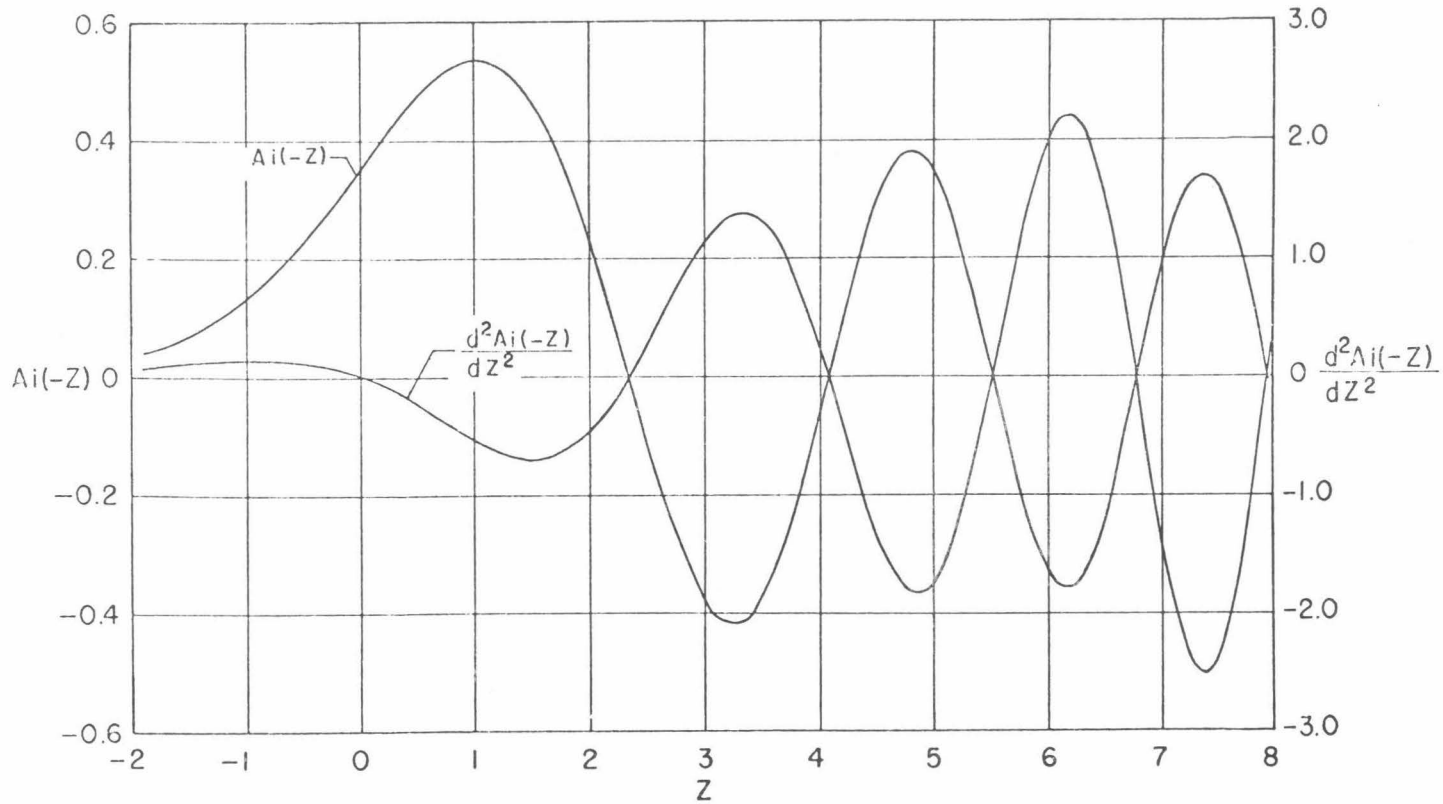

Figure 6.

Airy function Ai(-z) and its second derivative

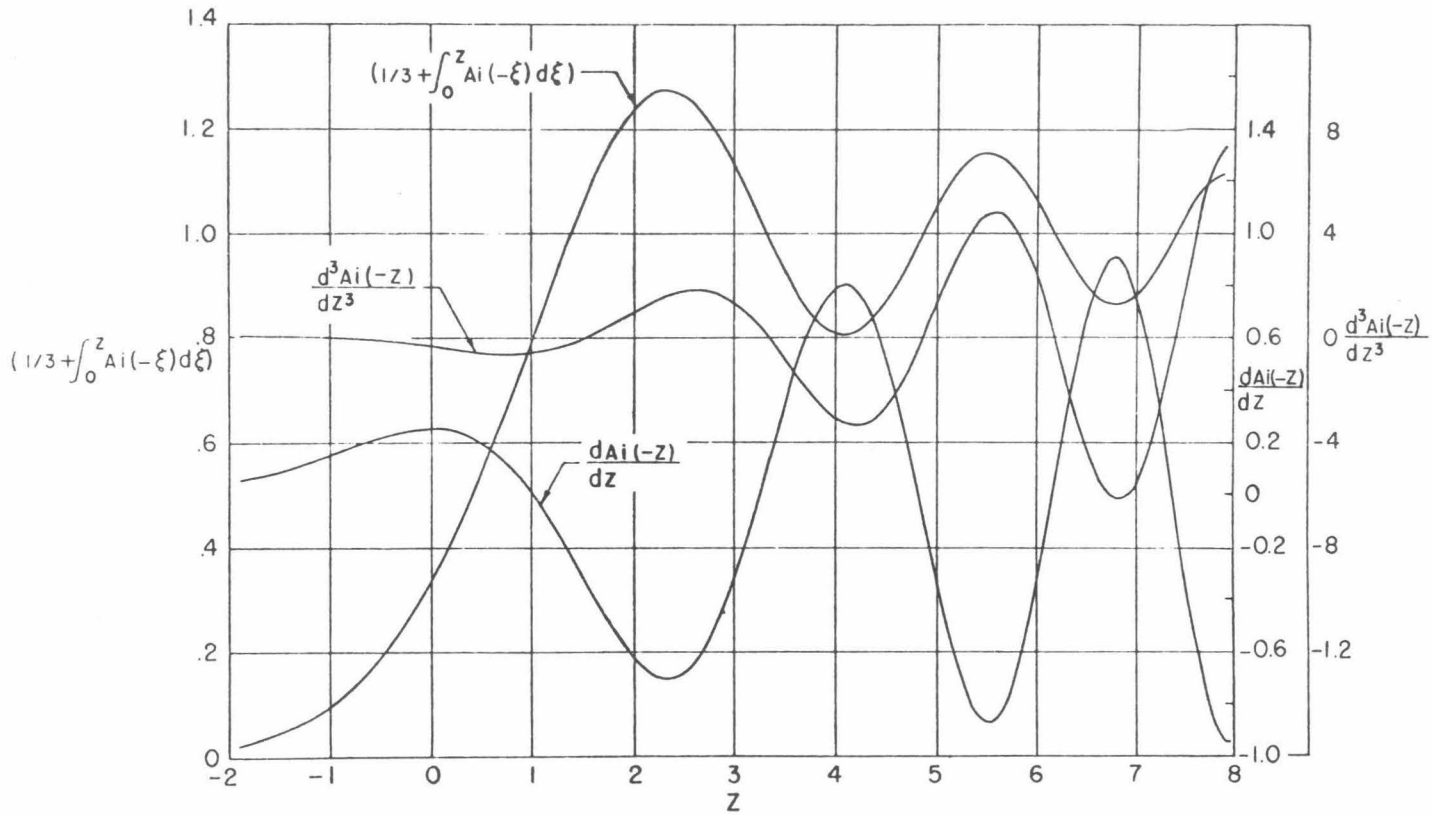

Figure 7

Airy integral, and first and third derivatives of Airy function Ai(-z)

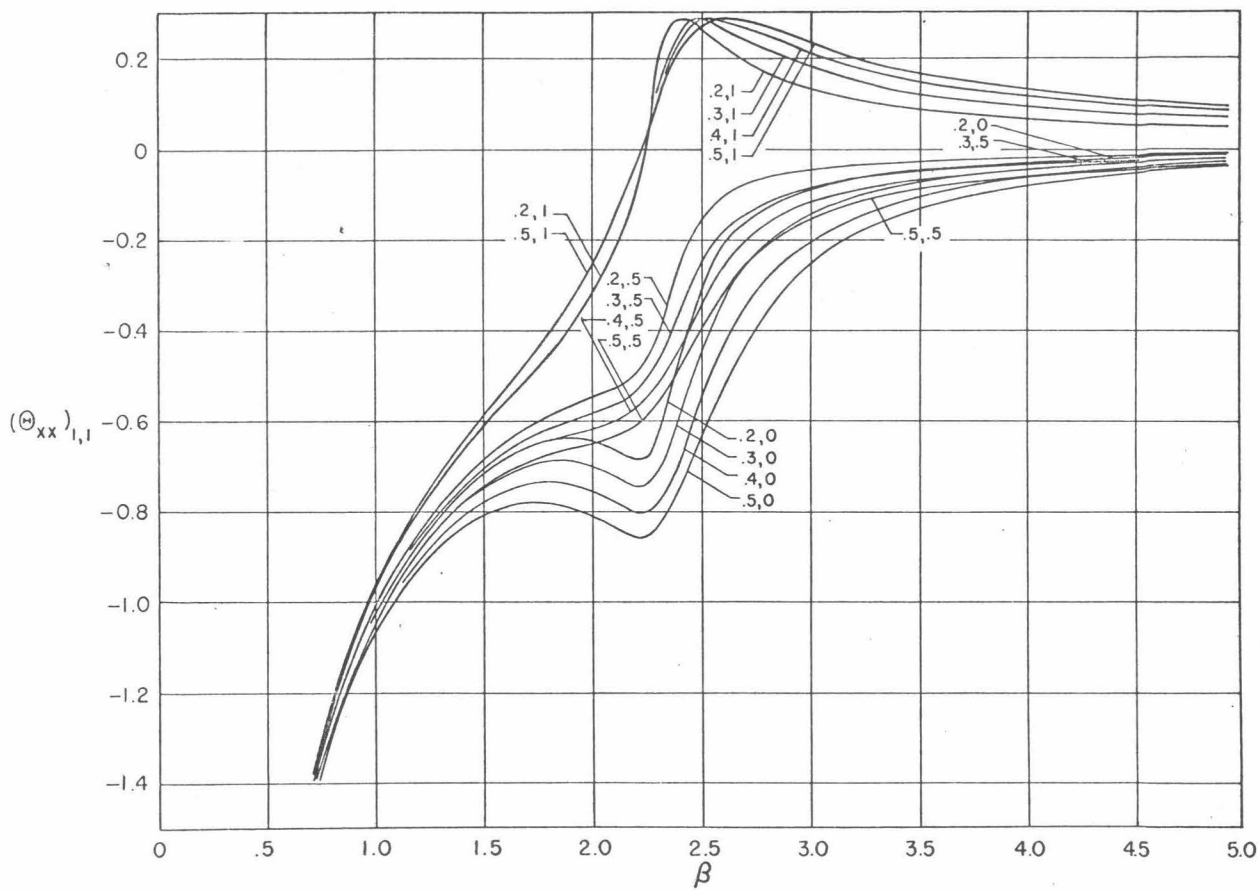

Figure 8(a)

Integrand functions $\theta(\alpha_{1,1}, Y, \beta)$ for real positive β; Y = 0, 0.5, and 1.0; and σ = 0.2, 0.3, 0.4, and 0.5

Also see Figures 8(b) and 8(c) pp. 29-30

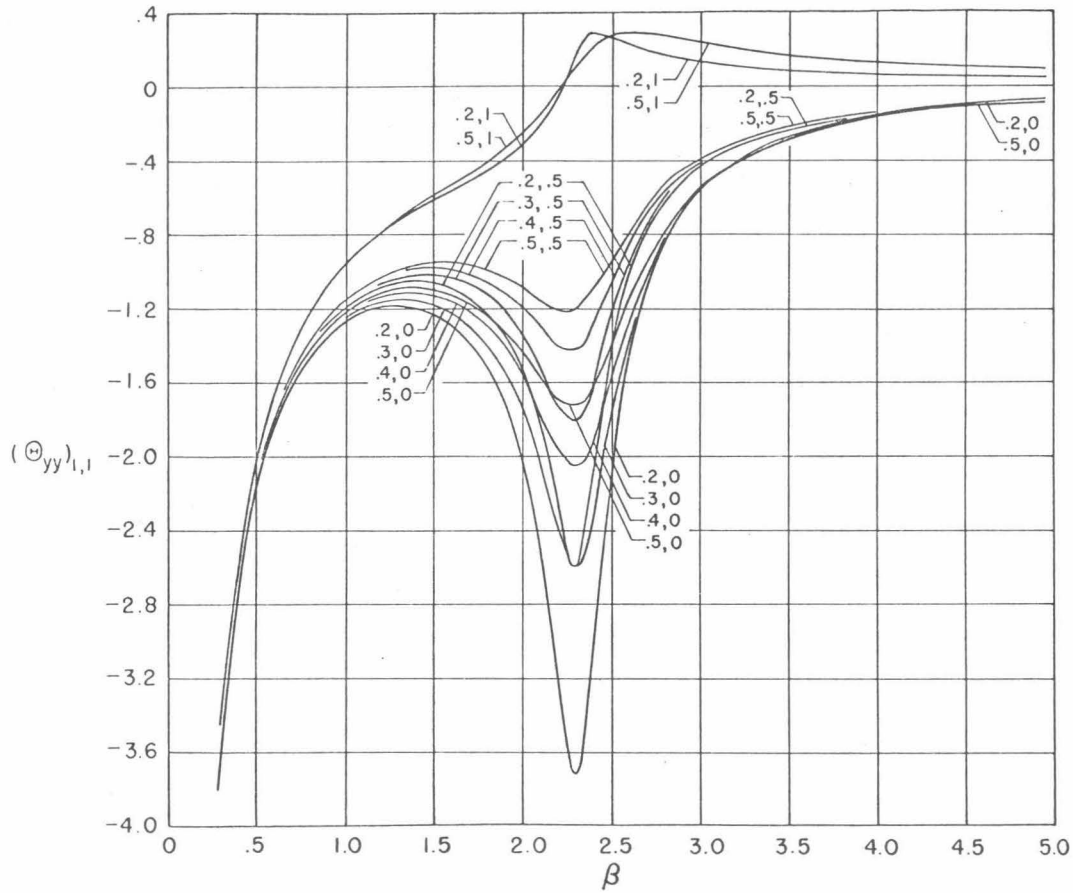
.4
0
-.4
-.8
-1.2
-1.6
-2.0
-2.4
-2.8
-3.2
-3.6
-4.0
$(\Theta_{yy})_{1,1}$
0
.5
1.0
1.5
2.0
2.5
3.0
3.5
4.0
4.5
5.0
β
.2,1
.5,1
.2,1
.5,1
.2,.5
.5,.5
.2,0
.5,0
.2,.5
.3,.5
.4,.5
.5,.5
.2,0
.3,0
.4,0
.5,0
.2,0
.3,0
.4,0
.5,0

Figure 8(b).

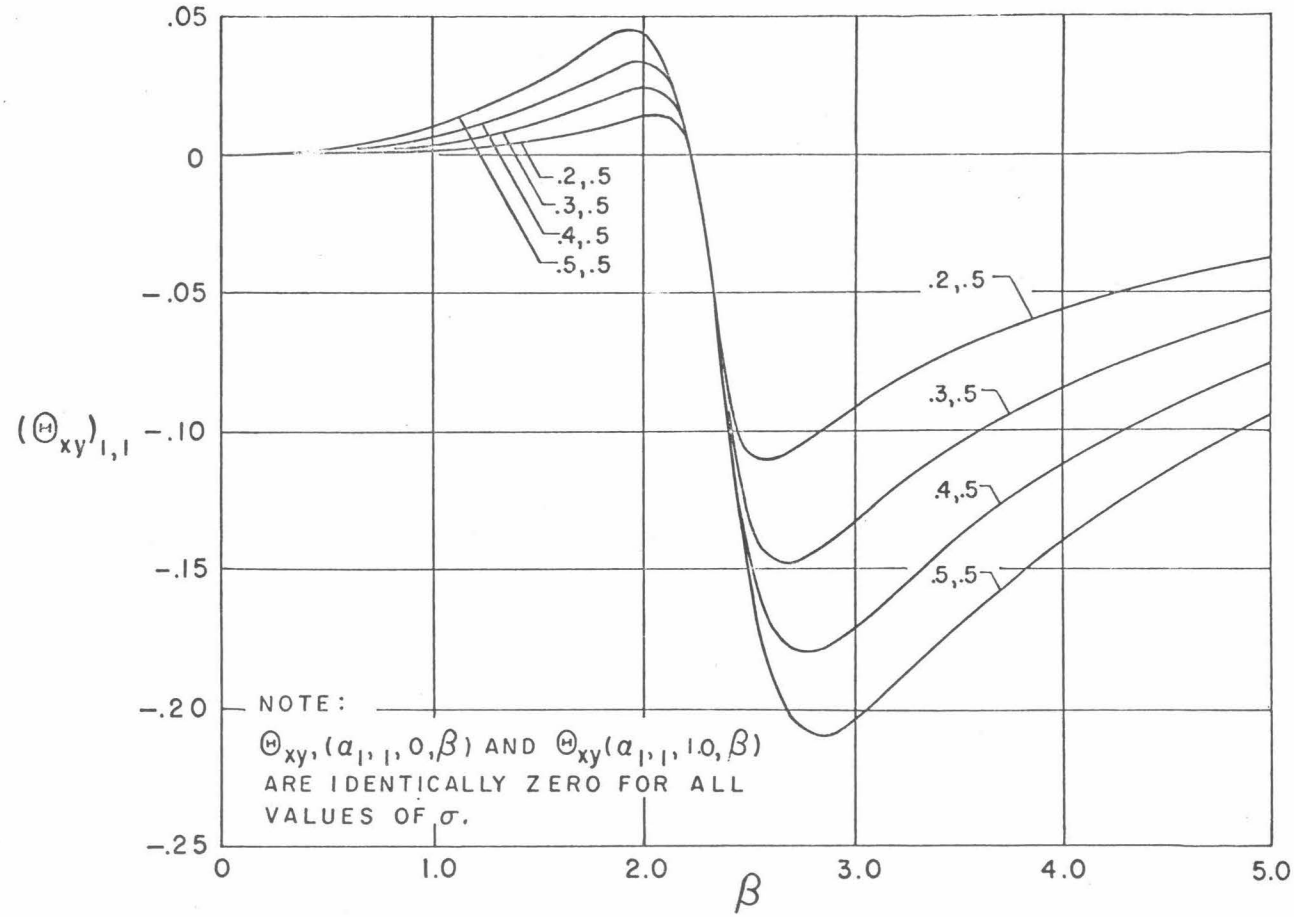
.05
0
-.05
-.10
-.15
-.20
-.25
$(\Theta_{xy})_{1,1}$
0
1.0
2.0
3.0
4.0
5.0
β
.2,.5
.3,.5
.4,.5
.5,.5
.2,.5
.3,.5
.4,.5
.5,.5
NOTE:
$\Theta_{xy}(\alpha_{1,1}, 0, \beta)$ AND $\Theta_{xy}(\alpha_{1,1}, 1.0, \beta)$
ARE IDENTICALLY ZERO FOR ALL
VALUES OF σ.

Figure 8(c).

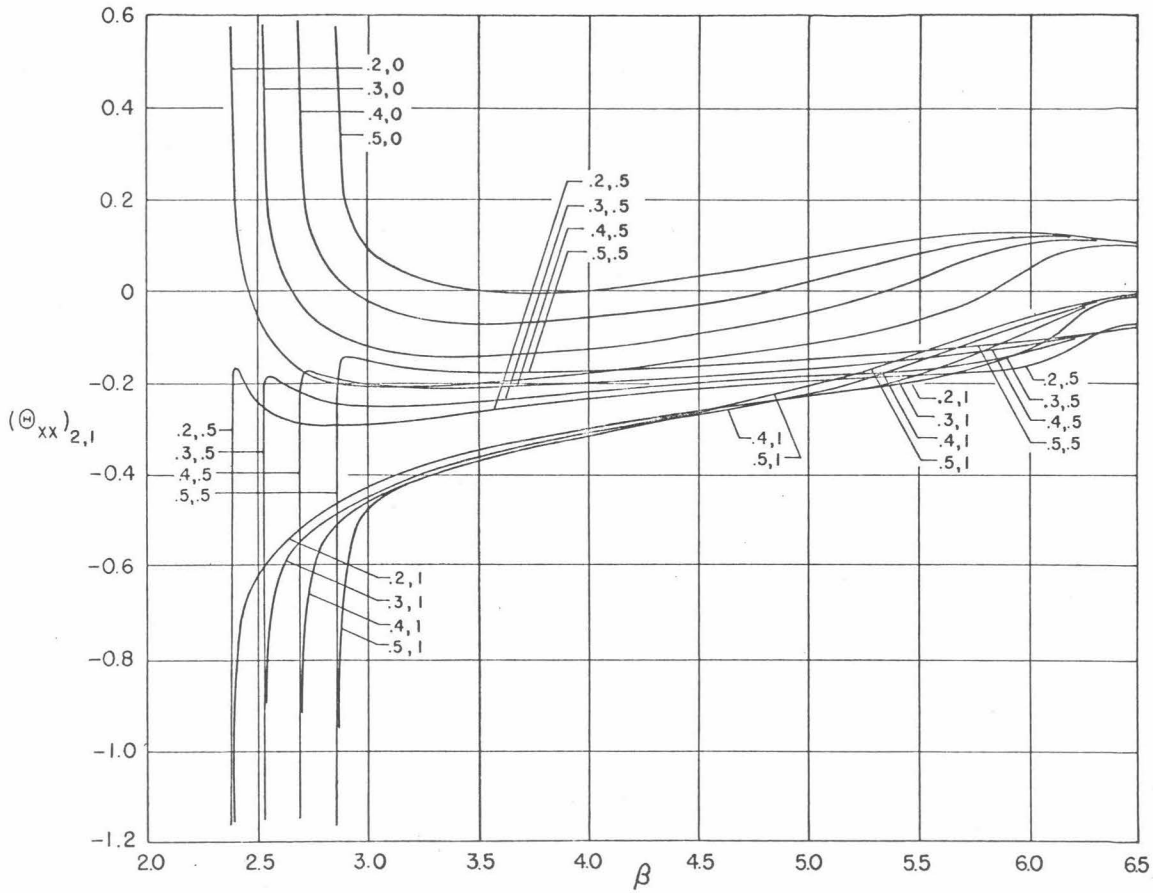

Figure 9(a).

Integrand functions $\Theta(\alpha_{2,1}, Y, \beta)$ in region of real positive β corresponding to real $\alpha_{2,1}$ for $Y = 0$, 0.5, and 1.0; and $\sigma = 0.2$, 0.3, 0.4, and 0.5

Also see Figures 9(b) and 9(c) pp. 32 and 33

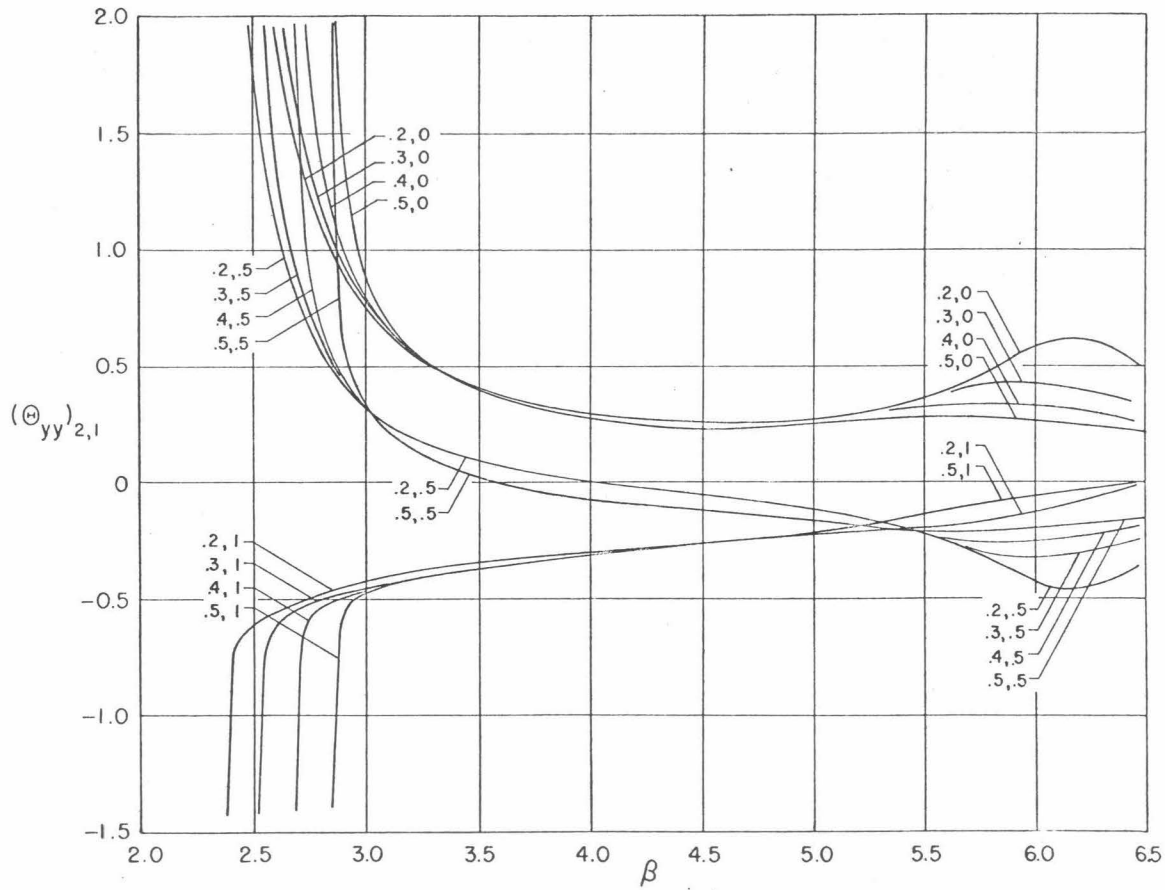
2.0
1.5
1.0
0.5
0
−0.5
−1.0
−1.5
2.0
2.5
3.0
3.5
4.0
4.5
5.0
5.5
6.0
6.5
β
$(\Theta_{yy})_{2,1}$
.2,0
.3,0
.4,0
.5,0
.2,.5
.3,.5
.4,.5
.5,.5
.2,1
.3,1
.4,1
.5,1

Figure 9(b).

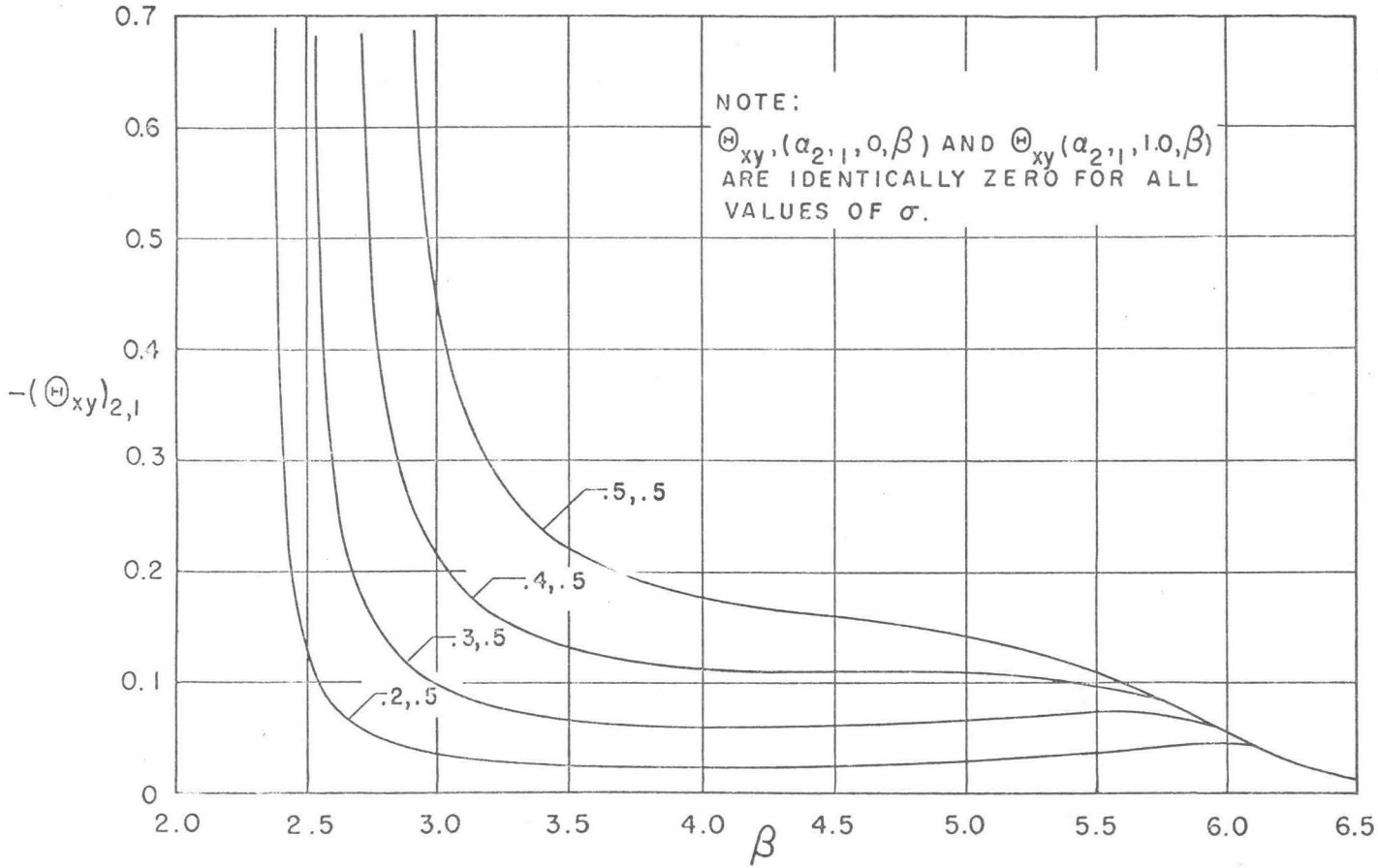
NOTE:
$\Theta_{xy}(\alpha_{2,1}, 0, \beta)$ AND $\Theta_{xy}(\alpha_{2,1}, 1.0, \beta)$ ARE IDENTICALLY ZERO FOR ALL VALUES OF σ.
$-(\Theta_{xy})_{2,1}$
β
.5,.5
.4,.5
.3,.5
.2,.5
0.7
0.6
0.5
0.4
0.3
0.2
0.1
0
2.0
2.5
3.0
3.5
4.0
4.5
5.0
5.5
6.0
6.5

Figure 9(c).

DISTRIBUTION LIST

6	Chief, Bureau of Naval Weapons, Wash. 25, D.C.	Code DLI-3	(1)
		RAAD-3	(1)
		RRRE	(1)
		RRRE-7	(1)
		RUAW-4	(2)
5	Chief, Bureau of Ships, Wash. 25, D.C.	Code 335	(1)
		421	(2)
		442	(1)
		644	(1)
3	Chief of Naval Research, Wash. 25, D.C.	Code 429	(1)
		438	(1)
		466	(1)
4	David Taylor Model Basin, Wash. 7, D.C.	Code 142	(1)
		500	(1)
		526	(1)
		591	(1)
1	Chief, Bureau of Yards and Docks, Wash. 25, D.C. (Research Div.)		
1	Naval Engineering Experiment Station, Annapolis, Md. (Librarian)		
1	Naval Academy, Annapolis, Md. (Librarian)		
1	Naval Postgraduate School, Monterey, Calif. (Librarian)		
1	Naval Weapons Laboratory, Dahlgren, Va. (Librarian)		
1	Naval Underwater Ordnance Station, Newport, R.I. (Librarian)		
2	Naval Ordnance Laboratory, Silver Springs, Md.		
		Desk HL (Library)	(1)
		Desk XL (Aeroballistics)	(1)
1	Naval Civil Engineering Laboratory, Port Hueneme, Calif. (Librarian)		
7	Naval Ordnance Test Station, Pasadena, Calif.	Code P508	(2)
		P804	(2)
		P8074	(1)
		P8076	(1)
		P80962	(1)
1	Naval Research Laboratory, Wash. 25, D.C. (Librarian)		
1	Navy Underwater Sound Laboratory, New London, Conn. (Librarian)		
1	Navy Electronics Laboratory, San Diego, Calif. (Librarian)		
1	Naval Air Development Center, Johnsville, Pa. (Librarian)		
1	Navy Mine Defense Laboratory, Panama City, Fla. (Librarian)		
1	Naval Ordnance Test Station, China Lake, Calif. (Code 7533)		
4	British Joint Services Mission (Naval Staff) via BuWeps DSC-3		
1	Defense Research Member (W), Canadian Joint Staff, via BuWeps DSC-3		
1	ASTIA Reference Center, Library of Congress, Wash. 25, D.C.		
6	Document Service Center, ASTIA, Arlington, Va.		
1	Office of Technical Services, Dept. of Commerce, Wash., D.C.		
6	National Aeronautics and Space Administration, Wash., D.C.		
1	National Bureau of Standards (Fluid Mechanics Div.) Wash., D.C.		
1	Coordinator for Research, Maritime Administration, Wash., D.C.		
1	National Science Foundation (Engr. Sciences Div.), Wash., D.C.		
1	Air research and Development Command, Wash., D.C.		
1	Air Force Office of Scientific Research (Mechanics Div.), Wash, D.C.		
1	Office of Ordnance Research, Durham, N.C.		
1	Committee on Undersea Warfare, NAS-NRC, Wash., D.C.		

1 Waterways Experiment Station, Vicksburg, Miss.
1 Merchant Marine Academy, Kings Point, L.I., N.Y. (Librarian)
2 Massachusetts Institute of Technology, Cambridge, Mass.
Dept. of N.A. and M.E., Prof. L. Troost (1)
Hydrodynamics Lab., Prof. A. Ippen (1)
1 Applied Physics Laboratory, Univ. of Washington, Seattle, Wash. (Librarian)
1 St. Anthony Falls Hydraulic Lab., Univ. of Washington, Seattle, Wash., (Librarian)
2 Stanford University, Stanford, Calif.
Dept. of Mech. Engr., Prof. B. Perry (1)
Head, Dept. of Math. (1)
1 Cornell University, Ithaca, N.Y. (Director, Grad. Sch. of Aero. Engr.)
2 Harvard University, Cambridge 38, Mass.
Dept. of Engr. Sci., Prof. G.F. Carrier (1)
Dept. of Math., Prof. G. Birkhoff (1)
1 University of Wisconsin Mathematical Research Center, Madison, Wisc. (Prof. L.M. Milne-Thomson)
1 Alden Hydraulic Laboratory, Worcester Polytechnic Institute, Worcester, Mass.
1 Garfield Thomas Water Tunnel, Ordnance Res. Lab., Penna. State University, University Park, Pa.
1 Davidson Laboratory, Stevens Institute of Technology, Hoboken, N.J.
1 The John Hopkins University, Baltimore, Md. (Dept. of Mech. Engr., Prof. S. Corrsin)
1 Colorado State University, Fort Collins, Colo. (Dept. of Civil Engr., Prof. M. Albertson)
2 University of Michigan, Ann Arbor, Mich.
Dept. of N.A. and M.E., Prof. R.B. Couch (1)
Dept. of Civil Engr., Prof. V. Streeter (1)
1 Polytechnic Institute of Brooklyn, Brooklyn, N.Y. (Head, Dept. of Aero. Engr. and Appl. Mech.)
2 Brown University, Providence, R.I., Div. of Appl. Math. (1)
Div. of Engr. (1)
2 Univ. of California, Berkeley, Calif., College of Engr.
Prof. A. Shade (1)
Prof. J.V. Wehausen (1)
1 Webb Institute of Naval Architecture, Glen Cove, L.I., N.Y. (Librarian)
1 New York State Maritime College, Fort Schuyler, N.Y. (Librarian)
1 University of Kansas, Lawrence, Kan. (Dean J.S. McNown)
1 Lehigh University, Bethlehem, Penna. (Dept. of Civil Engr., Prof. J.B. Herbich)
1 University of Notre Dame, Notre Dame, Indiana (Dept. of Engr. Mech., Prof. A.G. Strandhagen)
1 Rensselear Polytechnic Institute, Troy, N.Y. (Depth of Math., Prof. H. Cohen)
31 California Institute of Technology, Pasadena, Calif.
Prof. F. C. Lindvall (1)
Prof. D. Rannie (1)
Prof. C. B. Millikan (1)
Prof. M. S. Plesset (1)
Prof. T. Y. Wu (1)
Prof. V. A. Vanoni (1)
Hydrodynamics Lab. (25)

1 University of Illinois, Urbana, Ill. (Coll. of Engr., Prof. J. Robertson)
1 Scripps Institution of Oceanography, University of California, La Jolla, Calif. (Librarian)
1 Woods Hole Oceanographic Institution, Woods Hole, Mass. (Librarian)
1 Case Institute of Technology, Cleveland, Ohio (Librarian)
1 Institute of Fluid Mechanics and Applied Mathematics, University of Maryland, College Park, Md. (Librarian)
1 Philco Corporation, Philadelphia, Penna. (Engr. Librarian)
1 Vitro Corporation, Silver Springs, Md. (Engr. Librarian)
1 Gibbs and Cox, New York, N. Y. (Dr. S. Hoerner)

1 Hydronautics, Rockville, Md. (Mr. P. Eisenberg)
1 Technical Research Group, New York, N. Y. (Dr. P. Kaplan)
1 Aerojet General Corporation, Azusa, Calif. (Mr. J. Levy)
1 The Martin Company, Baltimore, Md. (Science Technical Librarian)
1 Lockheed Aircraft Corporation, Burbank, Calif. (Engr. Librarian)
1 Douglas Aircraft Company, El Segundo, Calif. (Mr. A. M. O. Smith)
1 Bell Aerosystems Company, Buffalo, N. Y. (Engr. Librarian)
1 McDonnel Aircraft Company, St. Louis, Mo. (Engr. Librarian)
1 Chance Vought Aircraft, Inc., Dallas, Texas (Engr. Librarian)
1 Republic Aviation Corporation, Farmingdale, L. I., N. Y. (Engr. Librarian)
1 EDO Corporation, College Point, N. Y. (Engr. Librarian)
1 The RAND Corporation, Santa Monica, Calif. (Librarian)
1 Electric Boat Division, General Dynamics Corporation, Groton, Conn. (Engr. Librarian)
1 Hydrodynamics Laboratory, Convair Division, General Dynamics Corp., San Diego, Calif.
1 Goodyear Aircraft Corporation, Akron, Ohio (Engr. Librarian)
1 Grumman Aircraft Engineering Corporation, Bethpage, L. I., N. Y. (Engr. Librarian)
1 Aeronutronic Division, Ford Motor Company, Newport Beach, Calif. (Engr. Librarian)
1 Southwest Research Institute, San Antonio, Texas (Dept. of Appl. Mech.)
1 Boeing Airplane Company, Seattle, Wash. (Aero-Space Librarian)
1 Hughes Tool Company, Culver City, Calif. (Librarian)
1 United Technology Corporation, Sunnyvale, Calif. (Dr. D. A. Rains)
2 Cleveland Pneumatic Industries, Inc., Advanced Systems Development Div., El Segundo, Calif. Mr. S. Thurston (1)
Mr. W. Ellsworth (1)
1 Westinghouse Electric Corporation, Baltimore Division, Friendship Int'l Airport, Md. (Engr. Librarian)
1 General Electric Corporation, Ordnance Dept., Pittsfield, Mass. (Engr. Librarian)
1 General Electric Corporation, LME Dept., Schenectady, N. Y. (Engr. Librarian)
1 Clevite Brush Development, Clevite Research Center, Cleveland, Ohio (Engr. Librarian)
1 AVCO Manufacturing Company, Everett, Mass. (Engr. Librarian)
1 Society of Naval Architects and Marine Engineers, New York, N. Y.
1 Applied Mechanics Reviews, New York, N. Y.
1 Engineering Societies Library, New York, N. Y.
1 Institute of the Aerospace Sciences Library, New York, N. Y.

6 E. P. Cochran, Jr., Commander, USN, Fluid Dynamics Branch, Office of Naval Research, Washington 25, D.C.
2 Mr. Dan Kallas, Material Laboratory, New York Naval Shipyard, Brooklyn, N. Y.
1 Laboratorio Hidrotecnico Salturnino de Brito, Rua Ferrieira Pontes 637, Rio de Janeiro, Brazil, Attn: Victor F. Motta